J. Membrane Biol. 71, 141–148 (1983)

The Journal of
Membrane Biology

# The Mechanism of Anion Transport Across Human Red Blood Cell Membranes as Revealed with a Fluorescent Substrate: I. Kinetic Properties of NBD-Taurine Transfer in Symmetric Conditions

O. Eidelman and Z.I. Cabantchik

Department of Biological Chemistry, The Hebrew University of Jerusalem, Institute of Life Sciences, 91904 Jerusalem, Israel

**Summary.** The molecular mechanism of anion exchange across the human red blood cell membrane was assessed with the fluorescent substrate analog NBD-taurine and the method of continuous monitoring of transport by fluorescence. The efflux of NBD-taurine was studied under a variety of experimental conditions such as temperature, pH and anion composition of cells and media. The temperature profile of NBD-taurine transfer from Cl-loaded cells into Cl media resembled that of Cl self-exchange, whereas that of NBD-taurine transfer from sulfate-loaded cells into sulfate media resembled that of sulfate self-exchange. Although the pH profiles of NBD-taurine transfer from Cl-loaded cells into Cl media and that of Cl self-exchange resembled each other, the analogous transfer with sulfate replacing Cl was markedly different. These and other data were analyzed and found to be consistent with a model which comprises the following: (a) a $H^+$-titratable group in the carrier mechanism; (b) alteration of transport sites between the two sides of the membrane (i.e., ping-pong kinetics); and (c) transmembrane distribution of transport sites which is modulated by pH. It is shown that NBD-taurine transfer represents a tracer flux of a fluorescent substrate which gives a measure for the presence of monovalent transport sites at the inner surface of the membrane. The latter is markedly affected by the relative concentrations of anions and $H^+$ on both sides of the red blood cell membrane.

**Key words:** anion exchange · fluorescent studies · membrane permeability · red blood cells

## Introduction

Transport mechanisms are classically studied in native systems with the aid of substrates which play a physiological role, with substrate analogs, and/or with chemical modifiers of diverse group specificity. For transport systems isolated in vesicles of high surface-to-volume ratio, the usage of natural substrates is limited by the speed at which compartments can be separated relative to transport rates, the efficiency of separation techniques, and the small intravesicular volume available for trapping radioisotopically labeled substrates.

A sensitive method for measuring transport, which provides a suitable alternative to classical methods – especially when dealing with isolated transport systems – has recently been developed [7, 8]. The method relies on the design of a fluorescent substrate whose fluorescence is quenched in one of the two compartments between which the transport occurs [6, 9]. Transport in the efflux mode is easily monitored in a continuous fashion as a time-dependent change in fluorescence intensity [9], thus circumventing the need for separating cells or vesicles from medium at different times. The method has been named CMTF[1], continuous monitoring of transport by fluorescence.

The successful application of CMTF to a particular transport system depends on the design of a substrate analog which has a fluorescent reporter group and which shows high specificity for the transport system. The introduction of NBD-taurine as a fluorescent substrate of the native anion transport system of human erythrocytes [9] and of the isolated band 3 membrane protein, the purported anion transporter, is an example of such an application. The fluorescence properties of the NBD moiety overlap largely with the absorption of hemoglobin which acts as a quencher of intracellular NBD-taurine [8]. For hemoglobin-free systems, anti-NBD antibodies can serve as efficient quenchers of extracellular or extravesicular NBD-taurine [6].

[1] *Abbreviations used:* CMTF, continuous monitoring of transport by fluorescence; DNDS, 4,4′-dinitro-2,2′-stilbenedisulfonic acid; HEPES, N-2-hydroxyethylpiperazine-N′-ethane sulfonic acid; HNBMG, hydroxynitrobenzyl-S-mercaptoguanosine; MES, 2[N-morpholino]ethane sulfonic acid; NBD-taurine, N(2-aminoethylsulfonate)-7-nitrobenz-2-oxa-1,3-diazole; NP-40, Nonidet P-40; PBS, phosphate-buffered saline (NaCl 147 mM, phosphate 20 mM, pH 7.4); TCA, trichloro-acetic acid; Tris, Tris(hydroxymethyl)amino-methane.

0022-2631/83/0021-0141 $01.60

In a preliminary study [9] the claim for specific transfer of NBD-taurine by the anion transport system rested on the use of classical inhibitors of anion exchange and on competition with the natural substrate $Cl^-$ for common transport sites. In this work we demonstrate by stricter criteria that the transfer of NBD-taurine across human red cell membranes is accomplished exclusively by the anion transport system. This transfer is interpreted as occurring via the monovalent form of the anion carrier. The kinetic analysis of NBD-taurine efflux profiles obtained in symmetric conditions with respect to anion content of cells and medium, at different temperatures and pH values, support the model of alternating sites [11, 19], referred to in carrier kinetics as a sequential mechanism [3] and in enzyme kinetics as a ping-pong mechanism [4]. The characteristics of anion transport as manifested in asymmetric conditions is the subject of the accompanying paper.

## Materials and Methods

NBD-taurine was synthesized as previously described [9]. DNDS and phloretin were obtained from K and K (ICN Pharmaceuticals). Tris base, MES and HEPES were purchased from Sigma Chemical Co. NP-40 was obtained from British Drug House (BDH), England. HNBMG was synthesized as previously described [1]. Persantin was a generous gift from Squibb Pharmaceuticals. [$^3$H]uridine and Na$^{36}$Cl were purchased from the Radiochemical Centre, Amersham, England. Other chemicals were of the best available grade.

### *Preparation of Chloride-Loaded Cells*

Red cells from freshly withdrawn blood or recently outdated blood (obtained from the Shaarei Zedek Medical Center, Jerusalem) were washed with PBS (148 mM NaCl, 20 mM phosphate, pH 7.4) until free of contaminating buffy coat. The cells were subsequently washed and resuspended in the medium of choice, as indicated.

### *Preparation of Sulfate-Loaded Cells*

Washed cells were incubated in sulfate medium (usually 100 mM $Na_2SO_4$, 20 mM phosphate, pH 7.4, or as otherwise indicated) at 3% hematocrit for a 30-min period at 37 °C. The cells were spun down, resuspended in sulfate medium, and the incubation procedure was repeated.

### *Change of Intracellular pH*

Chloride cells at 3% hematocrit were incubated for 1 hr at 37 °C in medium containing (mM): 75 NaCl, 75 KCl, 10 Tris base, 5 HEPES and 5 MES, and set to various pH values. Sulfate-loaded cells were incubated in similar media, except that 50 mM sulfate salts replaced the 75mM chloride salts. Incubations were repeated until the pH value of the supernate remained constant and was within 0.2 pH units of the set pH value. In the pH range 6.5 to 8.5, two successive incubations were usually sufficient for pH equilibration, whereas at more extreme pH ranges, three incubations were required.

### *Determination of Donnan Ratio and Cell Volume (at 30° C)*

Cells equilibrated in different media were brought to 10% hematocrit and incubated for an additional hour at 30 °C with [$^3$H]uridine (0.1 mM, $2\times10^5$ dpm/ml) and Na$^{36}$Cl ($2\times10^5$ dpm/ml). The cells were spun down, the supernate thoroughly withdrawn and saved. The cells were washed twice in an ice-cold stopping solution (mM: 100 $Na_2SO_4$, 20 phosphate, 0.1 DNDS, 0.1 phloretin, 0.1 persantine and 0.1 HNBMG, pH 8) and were finally lysed with distilled water. Supernates and lysates were counted for $^3$H and $^{36}$Cl after acid precipitation (TCA 5% final). The cell volume, $v_c$ ($\mu^3$/cell) was calculated as follows:

$$v_c = \frac{[^3\text{H}]\text{dpm (lysate)}}{[^3\text{H}]\text{dpm (sup)}} \cdot c \cdot \frac{1}{N} \tag{1}$$

where $c$ is a constant which takes into account the dilutions and conversion of units, and $N$ is the number of cells per cm$^3$ sample. The value of $N$ was calculated using the hemoglobin absorbance $A_{410}$ of cell lysates (50 µl cell suspension + 2 ml distilled water) and the conversion factor $5.5\times10^6$ cells/(ml $\times$ $A_{410}$). The latter factor was determined from the number of cells counted with a Coulter counter (Coulter Electronics, Dunstable, England) and hemoglobin reading of cell lysates obtained from the same cell suspension.

Donnan ratios were calculated as:

$$r = \frac{[^{36}\text{Cl}]\text{dpm (lysate)}}{[^3\text{H}]\text{dpm (lysate)}} \cdot \frac{[^3\text{H}]\text{dpm (sup)}}{[^{36}\text{Cl}]\text{dpm (sup)}}. \tag{2}$$

### *Continuous Monitoring of Transport by Fluorescence (CMTF)* [8]

Cells equilibrated with a given medium were incubated with NBD-taurine (1 mM) in the same medium for 1 hr at 37 °C (final hematocrit 10%, cell volume 50 µl). The suspension was gently bubbled with $N_2$ to remove $CO_2$, and was kept on ice. The cells were brought to and kept at the flux temperature under $N_2$ for 20 to 30 min prior to the flux measurement.

Extracellular NBD-taurine was removed by two successive washes of loaded cells (5 µl) with ice-cold isotonic $Na_2SO_4$ (1 ml), using an Eppendorf microfuge (12,000 × g, 4 sec). The final cell pellet was suspended in 0.5 ml ice-cold isotonic $Na_2SO_4$ and kept on ice. Fluxes were initiated by jetting 50 µl aliquots of cell suspensions into 4 cuvettes, each containing 2 ml medium, and placed in a water thermostated multi-cuvette holder of the spectrofluorimeter (Perkin-Elmer, MPF-4). Fluxes occurring simultaneously were recorded fluorimetrically by sequential positioning of the cuvettes in the light path. Standard fluorimeter settings were as follows: $\lambda_{exc}=478$ nm (5 nm slit); $\lambda_{em}=540$ nm (10 nm slit); dinode voltage 750 V (ratio mode). The flux solutions containing sulfate were thoroughly bubbled with $N_2$ prior to flux measurements, and the cell compartment was flushed with $N_2$ gas.

In several instances fluxes were monitored with a Fluorolog II double beam spectrofluorimeter (SPEX Industries, Metuchen, N.J.), equipped with a photon-counting detector and a Datamate microprocessor.

The total amount of NBD-taurine initially present in cells was obtained by adding a small aliquot of detergent NP-40 (0.025% wt/vol final) to the cell suspension at the termination

of the flux measurement. This value will be referred to as $F(\infty)$, fluorescence intensity at infinite time.

Rate constants $k$ ($min^{-1}$) of NBD-taurine efflux were determined as:

$$k=\frac{1}{F(\infty)-F(o)}\cdot\frac{dF}{dt}(t=0) \tag{3}$$

where $dF/dt$ $(t=0)$ is the initial slope of the fluorescence intensity change with time and $F(o)$ is the fluorescence at $t=0$.

Initial efflux rates $v$ (pmol/min/cell) were determined as:

$$v=\frac{dF}{dt}(t=0)\cdot\frac{f}{N} \tag{4}$$

where $df/dt$ $(t=0)$ is as stated above, $f$ is the calibrated conversion factor of fluorescence intensity to NBD-taurine concentration, and $N$ is the number of cells present in the cuvette, determined from $A_{410}$, as stated above. In order to compensate for the differences in the internal concentration $S_i$ of NBD-taurine at Donnan equilibrium at various pH values, the $v$ values were normalized to 1 mM NBD-taurine concentration ($\bar{v}=v/S_i=v/rS_o$), where $S_o=1$ mM. This correction is valid inasmuch as it has been shown that at 1 mM the apparent Michaelis constant of NBD-taurine $K_S \gg S_i$ [8].

## Results and Discussion

### *NBD-Taurine Efflux under "Symmetric" Conditions: Kinetic Profile*

The method used to study the efflux of NBD-taurine from NBD-taurine-loaded cells is based on the continuous monitoring of transport by fluorescence (CMTF) [8]. The change in fluorescence intensity corresponds to the increase in in concentration of NBD-taurine appearing in the extracellular space, thus reflecting the egress of probe from cells. Typical CMTF tracings of NBD-taurine egress from Cl-loaded cells into Cl medium and from $SO_4$-loaded cells into $SO_4$-medium are shown in Fig. 1. The flux measurements were performed on the Fluorolog II spectrofluorimeter and all data were stored into the Datamate microprocessor, with each data entry reflecting the fluorescence intensity accumulated during a 5-sec period.

The CMTF raw data is shown in Fig. 1A. Both sets of data are interpretable in terms of single exponential functions, as shown in the semilogarithmic plot of $[F(t)-F(0)]/[F(\infty)-F(o)]$ vs. time $(t)$ (Fig. 1 *B*), where $F(t)$, $F(o)$ and $F(\infty)$ are the fluorescence intensities at times $t$, $t=0$, and $t=\infty$, respectively (for experimental details, *see* Materials and Methods). That a single rate constant $k$ describes the kinetics of NBD-taurine efflux along the entire (>90%) profile is shown by the constancy of the instantaneous rate parameter $k(t)$ (Fig. 1 *C*) which is defined as:

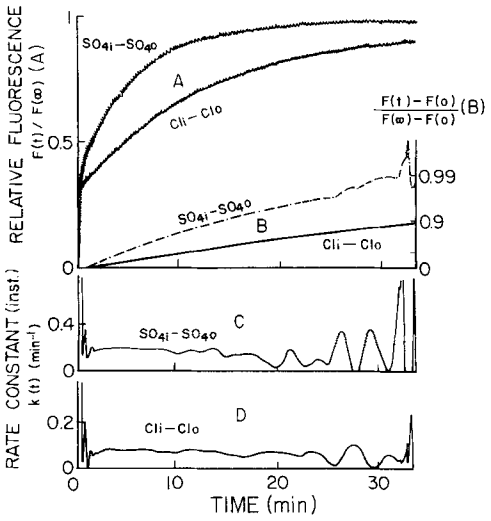


**Fig. 1.** NBD-taurine efflux under symmetric conditions. Red cells were pre-equilibrated at 30 °C in either chloride medium (150 mM NaCl, 10 mM HEPES, pH 7.4) or sulfate medium (110 mM $Na_2SO_4$, 10 mM HEPES) and were subsequently loaded with 1 mM of NBD-taurine in the same media. Efflux of fluorescent probe from either Cl-loaded cells ($Cl_i$) or sulfate-loaded cells ($SO_{4_i}$) into either chloride or sulfate medium ($Cl_o$ or $SO_{4_o}$ respectively) was followed by the CMTF method on a SPEX Fluorolog II instrument. The rise in fluorescence intensity at $t=0$, that occurs immediately after addition of cells, is contributed mostly by scattering of light due to the presence of red blood cells [8]. The time course of NBD-taurine efflux (*A*) is given in relative fluorescence units $F(t)/F(\infty)$, where $F(\infty)$ is the fluorescence intensity attained at $t\to\infty$. The logarithmic profile of efflux (*B*) was calculated from the above as $[F(t)-F(o)]/[F(\infty)-F(o)]$ versus time, where $F(t)$, $F(o)$ and $F(\infty)$ are the fluorescence intensities at times $t$, $t=0$ and $t\to\infty$, respectively. The logarithmic profile was used for determining the instantaneous rate parameter $k(t)=\frac{d}{dt}\ln[F(\infty)-F(t)]$. The instantaneous rate parameter $k(t)$ is essentially equal to the "rate constant" which would be calculated from the slope of $F(t)$ at time $t$, divided by $[F(\infty)-F(t)]$ (*C* and *D*)

$$k(t)=\frac{d}{dt}\ln[F(\infty)-F(t)]=\frac{-1}{F(\infty)-F(t)}\frac{d}{dt}F(t). \tag{5}$$

As the fluorescence intensity (i.e., NBD-taurine concentration) approaches a limiting value at infinite time, increasing fluctuations in the computed parameter become evident. This is because the experimental noise is highly amplified in the calculations based on Eq. (5), as a result of divisions by progressively smaller differences. As will be explained further in the text, the different instantaneous rate constants obtained in Cl − as compared to $SO_4$ − conditions resulted from differences both in the competitive effects of the two anions and in the cell volumes attained upon equilibrations.

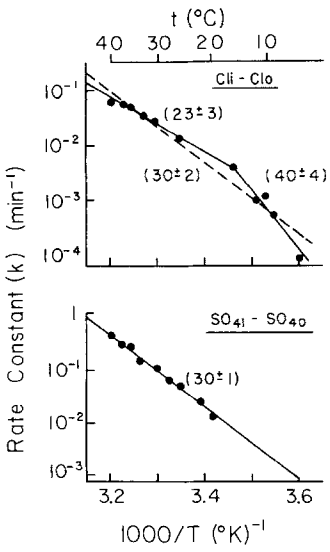


**Fig. 2.** Temperature dependence of NBD-taurine efflux under symmetric conditions. Red blood cells were pre-equilibrated either in chloride medium (150 mM NaCl, 10 mM HEPES, pH 7.4) or in sulfate medium (110 mM $Na_2SO_4$, 10 mM HEPES, pH 7.4) and then loaded with 1 mM NBD-taurine. The efflux of NBD-taurine into chloride or sulfate medium, respectively, was followed fluorimetrically by the CMTF method. Equilibration of cells with inorganic anions and with NBD-taurine as well as measurement of fluxes were performed as indicated in Fig. 1. *Upper figure:* Arrhenius plot of the rate constant of NBD-taurine efflux from Cl-loaded cells ($Cl_i$) into Cl medium ($Cl_o$). The continuous line is the nonlinear least-squares fit of the experimental data points to a biphasic linear form of two intersecting straight lines, yielding a break point ($T_b$) at 17 ±3 °C, and $E_a$ values of 23±3 kcal/mol (97±13 kJ/mol) above $T_b$ and 40±4 kcal/mol (168±17 kJ/mol) below $T_b$($r^2$ =0.992, $N$=12). The discontinuous line is the linear least-squares fit of the same data giving an $E_a$ of 30±2 kcal/mol (126±9 kJ/mol) ($r^2$=0.946). *Lower figure:* Arrhenius plot of the rate constants of NBD-taurine efflux from sulfate-loaded cells ($SO_{4i}$) into sulfate medium ($SO_{4o}$). The straight line is the linear least-squares fit of the experimental data points, which gives an $E_a$ of 30±1 kcal/mol (126 ±4 kJ/mol) ($r^2$=0.997, $N$=9)

*Temperature Dependence*

The efflux of NBD-taurine from Cl-loaded cells into Cl medium (pH 7.4) was determined by CMTF at various temperatures, as described in Materials and Methods. The corresponding rate constants of NBD-taurine efflux were calculated from the initial slope $(\Delta F/\Delta t)_i$ divided by the total fluorescence change between time 0 and ∞.

$$k = \frac{(\Delta F/\Delta t)_i}{F(\infty) - F(o)}. \quad (6)$$

The $k$ values were used for constructing the Arrhenius plot shown in Fig. 2 (top). Since the plot is of an apparent biphasic nature, the data were analyzed by a nonlinear regression program [17], assuming either monophasic or biphasic linear forms of the plot consisting of two intersecting lines and a "characteristic" (break) point. The biphasic form showed a temperature brake $T_b$ of 17±3 °C and respective $E_a$ values of 23± 3 kcal/mol (97±13 kJ/mol) and 40±4 kcal/mol (168±17 kJ/mol) above and below the break temperature ($r^2$ =0.992, $N$=12). The monophasic form gave an $E_a$ value of 30±2 kcal/mol (126± 9 kJ/mol) ($r^2$=0.946).

Similar studies performed with Br-loaded cells into Br medium (*not shown*) gave a break at 29±5 °C and $E_a$ values of 21±4 kcal/mol (88± 17 kJ/mol) and 27±1 kcal/mol (113±4 kJ/mol) above and below the break point, respectively. The biphasic temperature profiles of NBD-taurine efflux in Cl medium and Br medium, as well as the corresponding $E_a$ values and break points, are certainly in agreement with corresponding values obtained for Cl- and Br-self-exchange [2]: $E_a$=20±1 and 30±1 kcal/mol for Cl ($T_b$=15 °C); $E_a$=22 and 32 kcal/mol for Br ($T_b$=25 °C).

A similar study carried out on NBD-taurine transfer from sulfate-loaded cells into sulfate-containing medium is shown in Fig. 2 (bottom). Unlike in halide medium, the temperature profile in sulfate medium was demonstrably monophasic and was characterized by a single $E_a$ of 30± 1 kcal/mol(126±4 kJ/mol)($r^2$=0.997, $N$=9). This value is similar to that of 32 kcal/mol which was reported previously for sulfate self-exchange [15, 20].

The results shown above clearly indicate that the temperature profiles of NBD-taurine transfer measured in given conditions are essentially parallel to those obtained by tracer anion exchange measured under equivalent conditions. This supports the idea that both inorganic anion transfer and NBD-taurine transfer share common features of the underlying transport mechanism. However, they also suggest that the determining factor in the above profiles is not translocation of the fluorescent tracer but that the factor is one common to both inorganic and NBD-taurine transfer.

The recent analyses of biphasic Arrhenius plots by Silvius and McElhaney [22] cast some doubt on the classical interpretation of Arrhenius plots. The latter authors show that nonlinear Arrhenius plots arising from a variety of mechanisms, are better described by continuous "exponential breaking" (Eb) functions, rather than by two intersecting straight lines. We have therefore applied to our system the Eb function (class II mechanism) which deals with two temperature-

dependent reactions affecting the rate of transport, i.e., binding and translocation (Fig. 3). This is justified as it has been shown for Cl transport that the enthalpy of binding has a finite value [2], so that the Michaelis constant for Cl transport, $K_{Cl}$, is a temperature-dependent parameter $K_{Cl}(T)$. With this function applied to the data shown in Fig. 2, we obtained in Fig. 3 equally good or even better fit for the experimental points than with the classical analysis of two intersecting lines ($r^2=0.995$ in Fig. 3 as compared to $r^2=0.992$ in Fig. 2).

The analysis according to Silvius and McElhaney [22] postulates a characteristic temperature in the *Eb* function $T_c$ (Fig. 3), for which the temperature-dependent binding constant $K_s(T)$ equals the substrate concentration $S$ at which the temperature profiles are measured, i.e., $K_s(T_c)=[S]$. This applies to the case of Cl self-exchange for which $K_{Cl}(T_c)=150$ mM. The transfer of NBD-taurine in the presence of halides [9] is actually analogous to the case of a reaction in the presence of a competitive inhibitor $I$ which shows a temperature-dependent inhibitory constant $K_I(T)$. For the latter case, a characteristic temperature $T_c$ can also be postulated [22] such that for this $T_c$ the following relationship holds: $(1+[S]/K_s)=[I]/K_I(T)$ (i.e., $(1+[\text{NBD-t}]/K_{\text{NBD-t}})=[\text{Cl}]/K_{Cl}(T_c)$). As in the present experimental conditions $[\text{NBD-t}]<K_{\text{NBD-t}}$ [9], it follows that the $T_c$ for the temperature profile of NBD-taurine transfer coincides with the $T_c$ associated with the analogous profile of Cl self-exchange.

Since the same holds true also for other anions, we conclude that characteristic breaks found with NBD-taurine transfer reflect a limiting property determined by the interaction between the predominant anion in the system and the anion carrier. This interaction can take place not only with anion transport sites but also with the proposed anion modifier sites [14]. To what extent the break points result from transitions from one rate-limiting reaction to another or, as suggested by Brahm [2], they reflect a limiting property of carrier-substrate translocation, still remains to be shown.

### *pH Dependence*

The titratable carrier model of the anion exchange system [10] postulates that anion transport sites can exist either in a form responsible for translocation of monovalent anions (e.g. chloride form) or in a protonated form responsible for the translocation of divalent anions (e.g. sulfate form). In order to resolve whether NBD-taurine is transferred by the chloride or by the sulfate transport form of the anion carrier, we studied the pH profiles of NBD-taurine transfer in Cl as well as in $SO_4$ media (Fig. 4, top and bottom, respectively). Data are shown as relative fluxes in order to facilitate the comparison with the pH profiles of Cl self-exchange (modified from Brahm [2] and from Dalmark [5]) and of $SO_4$ self-exchange (modified from Schnell [21]). The results shown in Fig. 4 (top) display close similarities in the pH profile of NBD-taurine transfer in Cl media (at 30 °C) with those of Cl self-exchange at 38 °C [2] and at 0 °C [5]. In contrast, in $SO_4$ media, the profile of NBD-taurine transfer is distinctly different not only from that of sulfate self-exchange (Fig. 4, bottom) but also from that of Cl self-exchange and of NBD-taurine transfer measured in chloride media (Fig. 4, top). The data are compatible with the idea that NBD-taurine is transferred by the same carrier form which is responsible for monovalent anion exchange.

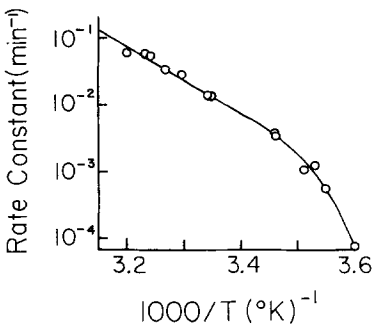


**Fig. 3.** Temperature dependence of NBD-taurine efflux from Cl-loaded cells into Cl medium: An alternative description of the characteristic break behavior. The experimental data points in the Arrhenius plot shown in Fig. 2 were analyzed by a non-linear least-squares fit (4 parameters) to Silvius' and McElhaney's [22] function:

$$\ln k = -\Delta E/RT - \ln\{1+\exp[\Delta(\Delta H^+)/R(1/T-1/T_c)]\}$$

where $k$ is the rate constant, $\Delta E$ is the activation energy, $\Delta H^+$ is the enthalpy of activation, $T$ the absolute temperature and $T_c$ the characteristic temperature (*see text*). The fit to this function (continuous line) gave an $r^2$ of 0.995 ($N=12$), whereas that of the two intersecting straight lines (Fig. 2) gave an $r^2=0.992$. The calculated parameters of the Eb function according to the model (ref. [22], Class II mechanisms, cf. Discussion) are: $E_a=23\pm1.5$ kcal/mol ($97\pm6$ kJ/mol), $\Delta(\Delta H^+)=70\pm10$ kcal/mol ($300\pm40$ kJ/mol), and the characteristic temperature is $10\pm1$° C

### *Interpretation of Experimental Data in Terms of a Kinetic Model*

In order to further discuss the present work, we have chosen to analyze the results within the

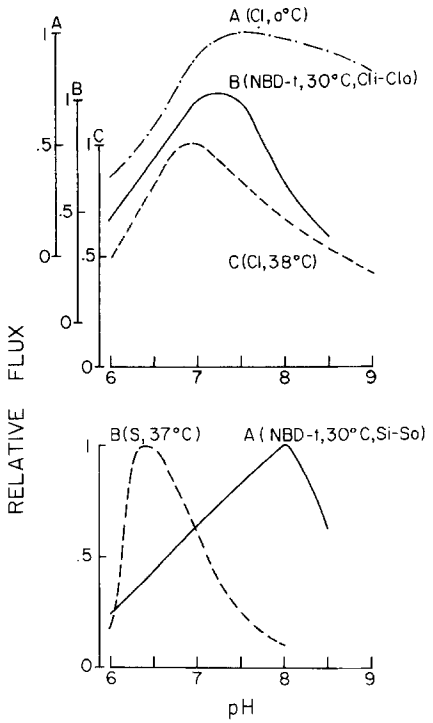


**Fig. 4.** pH dependence of NBD-taurine efflux under symmetric conditions. Red blood cells were pre-equilibrated either in chloride medium (mM: 150 NaCl, 10 Tris, 5 HEPES, 5 MES) or in sulfate medium (mM: 110 $Na_2SO_4$, 10 Tris, 5 HEPES, 5 MES) set to the indicated pH values, and subsequently loaded with 1 mM NBD-taurine. Efflux of fluorescent substrate into the same equilibration media was followed by the CMTF method (Fig. 1). Fluxes of anions are given in units relative to the respective flux values obtained at pH 7.0. *A. Upper figure:* The pH profile of NBD-taurine efflux from Cl-loaded cells into Cl medium (30 °C) (curve *B*). For comparison purposes we also show the pH profiles of Cl self-exchange at 0 °C (curve *A*, modified from ref. [5]) and at 38 °C (curve *C*, modified from ref. [2]). *B. Lower figure:* The pH profile of NBD-taurine efflux from $SO_4$-loaded cells into $SO_4$ medium (30 °C) (curve *A*). The pH profile of sulfate self-exchange at 37 °C (modified from ref. [21]) is shown in curve *B*

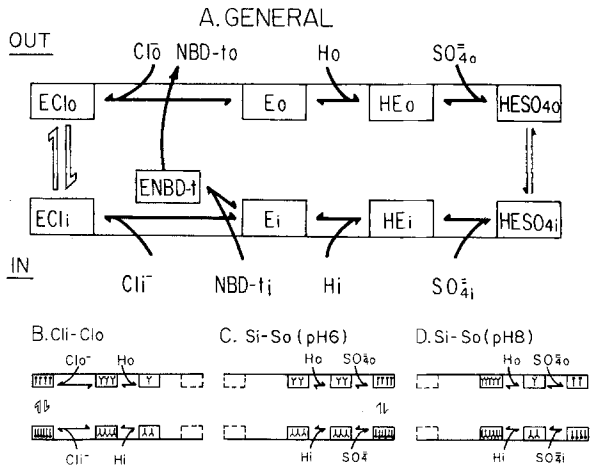


**Fig. 5.** Schematic model for anion exchange across the red cell membrane. *A. General scheme of the model:* The model incorporates basic elements which have been previously published [12], such as titratable transport groups [10], ping-pong kinetics [11] and transmembrane distribution of transport sites [5, 13]. *See also* refs. [3, 14] for reviews. The labels in the squares denote the various forms of the anion carrier *E* at the inner (*i*) or outer (*o*) face of the membrane. *HE* is the protonated form of the titratable carrier, while *E*Cl and *HE*$SO_4$ are the respective electroneutral carrier-anion complexes. Horizontal arrows represent bimolecular reactions of anions or protons with the carrier at the membrane interfaces. Vertical arrows represent translocation reactions of carrier-anion complexes across the membrane. The translocation of the *E*Cl complex is assumed to be much faster than that of *HE*$SO_4$ (right) and is denoted with the thick arrow. The carrier form responsible for binding NBD-taurine (NBD-t) is $E_i$ and the resulting translocating complex is *E*-NBD-$t_i$. *B–D. Schematic descriptions of distribution of carrier forms in various experimental conditions.* $Cl_i$, $SO_{4_i}$, Hi, $Cl_o$, $SO_{4_o}$ and Ho denote intracellular and extracellular chloride and sulfate and protons, respectively. The number of bars inside the squares gives a measure for the number of transport sites associated with the particular carrier form (as in *A*) at either the inner or outer membrane surface. *B. $Cl_i - Cl_o$ experimental conditions:* In these conditions the distribution of carrier forms between the two faces of the membrane is largely determined by the Donnan ratio (cf. Dalmark, ref. [5]). As pH increases, the concentration of $E_i$ is expected to increase, while that of $E_o$ is expected to decrease. On the other hand, the protonated forms of carrier are expected to decrease with an increase in pH. *C–D. $SO_{4_i} - SO_{4_o}$ conditions:* In these conditions the pH dependence of the distribution of carrier forms is expected to be distinctly different from that expected for $Cl_i - Cl_o$ conditions (*B*). In $SO_4$ conditions the protonated forms (*HE* and *HE*$SO_4$) become the carrier species relevant for sulfate transport. Thus, at relatively low pH (*C*), the concentration of both $E_i$ and $E_o$ are relatively low, while at relatively higher pH (*D*) the concentration of $E_i$ and $E_o$ are relatively larger. If NBD-t is transported by $E_i$ only, then the expectations are, therefore, that NBD-taurine efflux should markedly increase with pH

framework of the kinetic model displayed in Fig. 5. In this model we have incorporated some elements suggested in previous studies, such as the concept of titratable carrier [10] and the ping-pong mechanism [11]. The model rationalizes the pH profiles of anion self exchange and the obligatory exchange phenomenon [14], taking into account the effect of anion composition on the transmembrane distribution of transport sites [5, 13]. Two forms of carrier are assumed to be involved in anion transfer [10]: a form *E* responsible for the transfer of monovalent anions (e.g., $Cl^-$, $Br^-$, $F^-$, $NO_3^-$) and the protonated form *HE* responsible for the transfer of divalent anions (e.g., $SO_4^{-2}$, oxalate).

For simplicity's sake, the model shows sulfate binding to the HE form of the carrier, although recent work of Milanick and Gunn [18] suggests that sulfate can bind to *E* as well as to *HE*. For the present discussion, however, the order of binding of $H^+$ and $SO_4^{-2}$ to the carrier is not an essen-

tial feature as the fact that the major transportable form of sulfate is via the *HE* $SO_4$ form. The data shown in this work are consistent with the idea that NBD-taurine is transported by the *E* form. This emerges from the fact that under symmetric $Cl_i - Cl_o$ conditions (Fig. 4, top), the pH profile of NBD-taurine efflux is similar to that of Cl equilibrium exchange as measured by tracer $^{36}Cl$ efflux (Fig. 4, top *A*). On the other hand, under symmetric $SO_{4_i} - SO_{4_o}$ conditions, the pH profile of NBD-taurine efflux is distinctly different from that of sulfate equilibrium exchange (Fig. 4, bottom). These differences in pH behavior can be rationalized on the basis that the apparent competitive inhibition of sulfate on NBD-taurine decreases as pH is increased, whereas the competitive effect of Cl varies only slightly with pH. This is schematically portrayed in Fig. 5 (*C* and *D*) which shows that as the pH is increased from 6 to 8, the concentration of $E_i$ (the form which transfers NBD-taurine) also increases accordingly.

An essential point to be assessed is what part of the anion transport mechanism does NBD-taurine efflux actually measure? First, from the single exponential nature of the efflux profiles measured under symmetric conditions (Fig. 1), it is deduced that the concentration of NBD-taurine present in cells is considerably smaller than the apparent $K_m$ for this probe. Thus, NBD-taurine can have only a minor effect on the transmembrane distribution of the various carrier forms. Second, the rate of NBD-taurine efflux ($v$) depends both on the concentration of the ($E$-NBD-taurine)$_i$ complex and on the molecular rate constant $h_{io}^{\text{NBD-t}}$ for the translocation of the complex:

$$v = h_{io}^{\text{NBD-t}} [E\text{-NBD-t}]_i. \tag{7}$$

We assume also equilibrium of substrates with carrier forms at each one of the membrane surfaces. This assumption is justified because binding studies [16, 23] show that the rate of formation of inhibitor-carrier or substrate-carrier complexes are much shorter than the efflux rate followed by the CMTF method. We can therefore write:

$$v = h_{io}^{\text{NBD-t}} \frac{[E]_i \cdot [\text{NBD-t}]_i}{K_A} \tag{8}$$

where $K_A$ is the association constant of $[E\text{-NBD-t}]_i$. Thus, for a given concentration of NBD-taurine inside the cell, the initial rate of NBD-taurine efflux is proportional to the concentration of the $E_i$ form.

Third, the concentration of $E_i$ depends on the actual conditions of the system such as pH and anion composition of the two compartments, both of which affect the transmembrane distribution of carrier (Fig. 5) [5, 13]. An extreme example of skewed distribution of carrier forms was obtained with the asymmetric $Cl_i - SO_{4_o}$ or $SO_{4_i} - Cl_o$ systems (*see* accompanying paper). This distribution resulted from the obligatory nature of anion exchange and the asymmetric conditions imposed on the system. It should be stressed that factors such as pH and temperature might have affected $v$ also by modification of $K_A$, the affinity of the probe for *E*. However, the fact that both the pH and the temperature profile of NBD-taurine flux were markedly different in Cl as compared to $SO_4$ conditions (Fig. 4), indicates that the alleged effects on $K_A$ are considerably smaller than those of pH on $E_i$ and those of temperature on $h_{io}^{\text{NBD-t}}$ (Eq. 8).

Finally, the similarity between the temperature profiles of NBD-taurine transfer measured in various inorganic media and those of inorganic anion exchange measured in virtually similar media is also in line with the above idea that NBD-taurine transfer provides a measure for the kinetic status of the anion transport system, as affected by pH, temperature and anion composition. This clearly underscores the reliability of the probe NBD-taurine as a substrate of anion transport systems and the versatility of CMTF as an analytical tool for studying transport mechanisms. Further aspects of the anion transport system as studied with CMTF under asymmetric conditions is the subject of the accompanying paper.

This work was supported in part by grants from the PHS, N.I.H. (R01GM 27753), and from the United States-Israel Binational Science Foundation, Jerusalem. The technical assistance of Ms. M. Zangvill and Ms. Y. Keren-Zur is kindly appreciated. We gratefully acknowledge Profs. H. Ginsburg and W.D. Stein, and Mrs. A. Darmon for helpful suggestions, as well as Ms. E. Dicker for typing the manuscript. The spectrofluorimeter Fluorolog II used in this work was a gift of S. and E. Neidorff, I. and S. Scheinman and their friends in memory of S. Brickman.

A preliminary account of this work was presented at the Israel Biochemical Society Annual Meeting, 1982, Rehovot, Israel, *Isr. J. Med. Sci.* **18**:*S*11

## References

1. Bibi, O., Schwartz, J., Eilam, Y., Shohami, E., Cabantchik, Z.I. 1978. Nucleoside transport in mammalian cell membranes: IV. Organomercurials and organomercurial-mercaptonucleoside complexes as probes for nucleoside trans-

port systems in hamster cells. *J. Membrane Biol.* **39**:159–183
2. Brahm, J. 1977. Temperature-dependent changes of chloride transport kinetics in human red cells. *J. Gen. Physiol.* **70**:283–306
3. Cabantchik, Z.I., Knauf, P.A., Rothstein, A. 1978. The anion transport system of the red blood cell: The role of membrane protein evaluated by the use of 'probes'. *Biochim. Biophys. Acta* **515**:239–302
4. Cleland, W.W. 1963. The kinetics of enzyme-catalyzed reactions with two or more substrates or products: I. Nomenclature and rate equations. *Biochim. Biophys. Acta* **67**:104–137
5. Dalmark, M. 1975. Chloride transport in human red cells. *J. Physiol. (London)* **250**:39–64
6. Darmon, A., Eidelman, O., Cabantchik, Z.I. 1982. A method for measuring anion transfer across hemoglobin-free cells and vesicles by continuous monitoring of fluorescence. *Anal. Biochem.* **119**:313–321
7. Eidelman, O., Cabantchik, Z.I. 1980. NBD-taurine transfer across membranes. *In:* Membrane Transport in Erythrocytes. U.V. Lassen, H.H. Ussing, and J.O. Wieth, editors. pp. 531–538. Munksgaard, Copenhagen
8. Eidelman, O., Cabantchik, Z.I. 1980. A method for measuring anion transfer across red cell membranes by continuous monitoring of fluorescence. *Anal. Biochem.* **106**:335–341
9. Eidelman, O., Zangvill, M., Razin, M., Ginsburg, H., Cabantchik, Z.I. 1981. The anion transfer system of erythrocyte membranes: NBD-taurine, a fluorescent substrate analog of the system. *Biochem. J.* (Molecular Aspects) **195**:503–513
10. Gunn, R.B. 1972. A titratable carrier model for both mono- and di-valent anion transport in human red blood cells. *In:* Oxygen Affinity of Hemoglobin and Red Cell Acid-Base Status. M. Rorth and P. Astrup, editors. pp. 823–827. Munksgaard, Copenhagen
11. Gunn, R.B., Frohlich, O. 1979. Asymmetry in the mechanism for anion exchange in human red blood cell membranes: Evidence for reciprocating sites that react with one transported anion at a time. *J. Gen. Physiol.* **74**:351–374
12. Jennings, M.L. 1978. Characteristics of $CO_2$-independent pH equilibration in human red blood cells. *J. Membrane Biol.* **40**:365–391
13. Jennings, M.L. 1980. Apparent 'recruitment' of $SO_4$ transport sites by the Cl gradient across the human erythrocyte membrane. *In:* Membrane Transport in Erythrocytes. U.V. Lassen, H.H. Ussing, and J.O. Wieth, editors. pp. 450–463. Munksgaard, Copenhagen
14. Knauf, P.A. 1979. Erythrocyte anion exchange and the band 3 protein: Transport kinetics and molecular structure. *Curr. Top. Membr. Transp.* **12**:249–363
15. Lepke, S., Passow, H. 1971. The permeability of the human red blood cell to sulfate ions. *J. Membrane Biol.* **6**:158–182
16. Macara, I.G., Cantley, L.C. 1981. Interaction between transport inhibitors at the anion binding sites of the band 3 dimer. *Biochemistry* **20**:5095–5105
17. Marquardt, D.W. 1963. An algorithm for least-squares estimation of non-linear parameters. *J. Soc. Indust. Appl. Math.* **11**:431–441
18. Milanick, M.A., Gunn, R.B. 1982. Proton-sulfate co-transport: Mechanism of $H^+$ and sulfate addition to the chloride transporter of human red blood cells. *J. Gen. Physiol.* **79**:87–113
19. Passow, H., Kampmann, L., Fasold, H., Jennings, M., Lepke, S. 1980. Mediation of anion transport across the red blood cell membrane by means of conformational changes of the band 3 protein. *In:* Membrane Transport in Erythrocytes. U.V. Lassen, H.H. Ussing, and J.O. Wieth, editors. pp. 345–372. Munksgaard, Copenhagen
20. Schnell, K.F. 1972. On the mechanism of inhibition of the sulfate transfer across the human erythrocyte membrane. *Biochim. Biophys. Acta* **282**:265–276
21. Schnell, K.F., Gerhardt, S., Schöppe-Fredenburg, A. 1977. Kinetic characteristics of the sulfate self-exchange in human red blood cells and red blood cell ghosts. *J. Membrane Biol.* **30**:319–350
22. Silvius, J.R., McElhaney, R.N. 1981. Non-linear Arrhenius plots and the analysis of reaction and motional rates in biological membranes. *J. Theor. Biol.* **88**:135–152
23. Verkman, A.S., Dix, J.A., Salomon, A.K. 1982. Anion transport inhibitor binding to band 3 in red blood cell membranes. *J. Gen. Physiol.* (*in press*)

Received 28 April 1982; revised 19. August 1982